Conf-911079--19

Heavy-Section Steel Irradiation Program: Embrittlement Issues*

W. R. Corwin

Oak Ridge National Laboratory
Oak Ridge, Tennessee 37831

CONF-911079--19

DE92 005424

ABSTRACT

Maintaining the integrity of the reactor pressure vessel (RPV) in a light-water-cooled nuclear power plant is crucial in preventing and controlling severe accidents and the potential for major contamination releases. The RPV is one of only two major safety-related components of the plant for which a duplicate or redundant backup system does not exist. It is imperative to understand and predict the capabilities and limitations of its integrity. In particular, it is vital to fully understand the degree of irradiation-induced degradation of the RPV's fracture resistance which occurs during service, since without that radiation damage it is virtually impossible to postulate a realistic scenario which would result in RPV failure. For this reason, the Heavy-Section Steel Irradiation (HSSI) Program has been established by the U.S. Nuclear Regulatory Commission (USNRC) to provide a thorough, quantitative assessment of the effects of neutron irradiation on the material behavior, and in particular the fracture toughness properties, of typical pressure vessel steels as they relate to light-water reactor pressure-vessel integrity. Effects of specimen size, material chemistry, product form and microstructure, irradiation fluence, flux, temperature and spectrum, and postirradiation annealing are being examined on a wide range of fracture properties including fracture toughness (K_{Ic} and J_{Ic}), crack arrest toughness (K_{Ia}), ductile tearing resistance (dJ/da), Charpy V-notch (CVN) impact energy, dropweight nil-ductility temperature (NDT), and tensile properties. Models based on observations of radiation-induced microstructural changes using the field ion microprobe and the high resolution transmission electron microscope provide improved bases for extrapolating the measured changes in fracture properties to wider ranges of irradiation conditions. The principal materials examined within the HSSI program are high-copper welds since their postirradiation properties are most frequently limiting in the continued safe operation of commercial RPVs. In addition, a limited effort focuses on stainless steel weld-overlay cladding, typical of that used on the inner surface

---

*Research sponsored by the Office of Nuclear Regulatory Research, U.S. Nuclear Regulatory Commission under Interagency Agreement DOE 1886-8109-8L with the U.S. Department of Energy under Contract DE-AC05-84OR21400 with Martin Marietta Energy Systems, Inc.

of RPVs, since its postirradiation fracture properties have the potential for strongly affecting the extension of small surface flaws during overcooling transients.

Recent results are described concerning the shifts in fracture toughness and crack arrest toughness in high-copper welds, the effects of irradiation on stainless-steel weld-overlay cladding, the unirradiated examination of a low upper-shelf (LUS) weld from the Midland reactor, irradiation temperature effects on Charpy and tensile properties of several LUS welds, initial theoretical studies related to irradiation-rate effects, and the continued investigation into the causes of accelerated low-temperature embrittlement recently observed in RPV support steels.

PROGRAM SCOPE AND GOALS

It is vital to fully understand the degree of irradiation-induced degradation of the RPV's fracture resistance which occurs during service, since without that radiation damage it is virtually impossible to postulate a realistic scenario which would result in RPV fracture. For this reason, the HSSI program has been established with its primary goal to provide a thorough, quantitative assessment of the effects of neutron irradiation on the material behavior, and in particular the fracture toughness properties, of typical pressure vessel steels as they relate to light-water reactor pressure-vessel integrity. Results from the HSSI studies will be integrated to aid in resolving major regulatory issues facing the USNRC which involve RPV irradiation embrittlement such as pressurized-thermal shock, operating pressure-temperature limits, low-temperature overpressurization, and the specialized problems associated with LUS welds. Taken together the results of these studies also provide guidance and bases for evaluating both the aging behavior and the potential for plant life extension of light-water reactor pressure vessels.

The HSSI program includes the direct continuation of irradiation studies previously conducted within the Heavy-Section Steel Technology (HSST) program augmented by enhanced examinations of the accompanying microstructural changes. Effects of specimen size, material chemistry, product form and microstructure, irradiation fluence, flux, temperature and spectrum, and postirradiation annealing are being examined on a wide range of fracture properties. The HSSI Program is arranged into 9 tasks: (1) program management, (2) K_{Ic} curve shift in high-copper welds, (3) K_{Ia} curve shift in high-copper welds, (4) irradiation effects on cladding, (5) K_{Ic} and K_{Ia} curve shifts in LUS welds, (6) irradiation effects in a commercial LUS weld, (7) microstructural analysis of irradiation effects, (8) in-service aged material evaluations, and (9) correlation monitor materials. Recent results and plans for each technical task are described in the following sections.

K_{Ic} CURVE SHIFTS IN HIGH-COPPER WELDS

In the fracture mechanics integrity analysis of RPVs, the initiation and arrest fracture toughness curves as described in Sect. XI of the *ASME Boiler and Pressure Vessel Code* are often used. These curves are also used for the normal operation of RPVs. The effects of neutron irradiation on toughness are accounted for by shifting the curves upward in temperature without change in shape by an amount equal to the shift (plus a margin term) of the CVN impact energy curve at the 41-J level. Such a procedure implies that the shifts in the fracture toughness curves

are the same as those of the CVN 41-J energy level, and that irradiation does not change the shapes of the fracture toughness curves.

The objectives of the HSSI Fifth Irradiation Series are to determine the K_{Ic} curve shifts and shapes for two irradiated high-copper, 0.23 and 0.31 wt %, submerged-arc welds (72W and 73W, respectively). All planned unirradiated and irradiated testing for the Fifth Irradiation Series has been completed. The irradiations were performed by the Oak Ridge National Laboratory (ORNL) at the Oak Ridge Research Reactor (ORR) at a nominal temperature of 288°C to average fluences of about 1.5×10^{19} neutrons/cm^2 (>1 MeV). Tests were performed by both ORNL and Materials Engineering Associates, Inc., and included tensile, CVN impact, drop-weight, and fracture toughness. Unirradiated compact specimens of 25-, 51-, 102-, 152-, and 203-mm thickness (1T, 2T, 4T, 6T, and 8TC(T), respectively) were tested, whereas irradiated testing was limited to 1T, 2T, and 4TC(T) specimens.

The results of testing have been presented previously.[1] For the CVN results, the 41-J transition temperature shifts using Weibull-based analyses were very similar to those obtained from hyperbolic or exponential curve-fitting techniques for the 72W and 73W welds. The 41-J shifts were 72 and 82°C, while the 68-J shifts were 82 and 105°C for welds 72W and 73W, respectively. The analyses also indicated that variations in neutron fluence did not influence the shifts or the shapes of the irradiated curves and, therefore, will allow for conclusions concerning effects of irradiation on curve shape.

The first step in the analysis was to evaluate the fracture toughness data to establish the data base appropriate for statistical analyses. For those specimens which met the E 399 criteria for a valid K_{Ic}, the K_{Ic} value is used. For those specimens which exhibited curvature in the load-displacement record, indicative of plastic deformation and, perhaps, stable ductile tearing, the K_{Jc} value was used. Because the data base includes results from both linear-elastic and elastic-plastic fracture mechanics calculations, the fracture toughness data have been designated K_{cl} for cleavage fracture toughness.

An unexpectedly large number of cleavage pop-ins in the irradiated specimens required examination of those results. Out of 156 unirradiated compact specimens, only two exhibited pop-ins. For the 110 irradiated specimens, however, 28 specimens exhibited a total of 36 pop-ins. For a number of previously stated reasons,[2] only the initial pop-in was used herein to determine cleavage fracture toughness for those specimens exhibiting pop-ins. Pop-ins of any size representing a cleavage event in the specimen were considered significant. Figure 1 shows a plot of cleavage fracture toughness for weld 72W in the irradiated condition. Each datum plotted represents one test specimen (the abscissa is not scaled). As shown, the pop-in results fit generally within the scatter bands of the fracture results and the lowest values are mixed between pop-ins and fracture results. These results suggest that cleavage pop-ins are significant relative to indicating propensity for cleavage fracture in the test specimen.

The K_{Ic} curve in Sect. XI of the ASME Code is a lower boundary to the data used for its development.[3] Three-parameter nonlinear regression analyses were performed for 72W and 73W in both the unirradiated and irradiated conditions using the simple exponential form of the ASME K_{Ic} curve. Various intercept values were obtained but statistical analyses revealed that they did not differ significantly from the ASME value of 36.48; thus, the intercept value was fixed at 36.48 MPa$\sqrt{m}$. Mean curve fits from the subsequent two-parameter nonlinear regression analyses gave fracture toughness temperature shifts, measured at the 100 MPa$\sqrt{m}$-level, of about 94 and 100°C for 72W and 73W, respectively, the same results obtained from the three-parameter

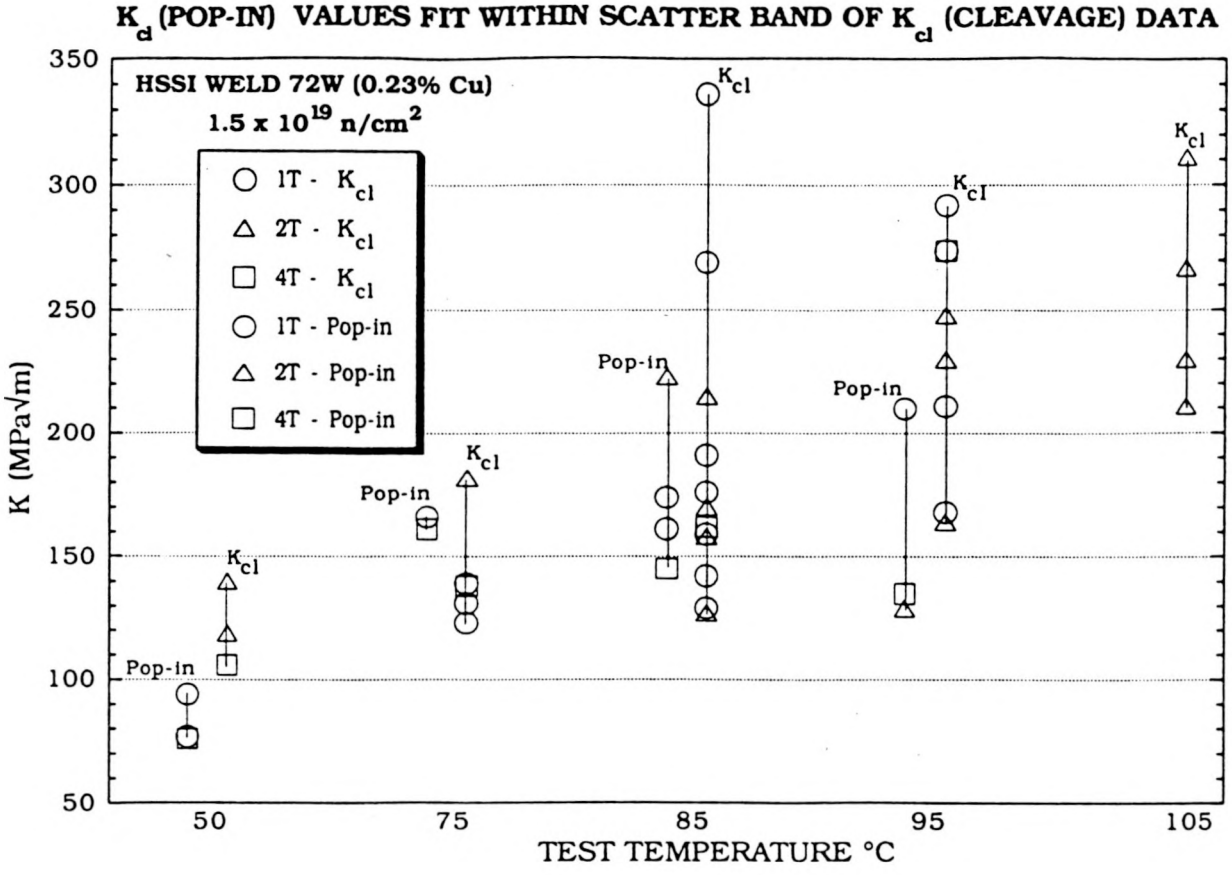

Fig. 1. Cleavage fracture toughness for irradiated HSSI weld 72W comparing first pop-in events with fracture toughness results from fracture events at the same test temperature. Each datum represents one specimen.

nonlinear regression analyses. Additionally, two-parameter analyses with the intercept equal to zero were performed and the results were similar to those discussed above.

In order to better examine changes in shape of the curve, the model was linearized. The fracture toughness 100-MPa√m temperature shifts are about 83 and 99°C for 72W and 73W, respectively. The analyses show some decreases in slopes for the irradiated data for both welds. These decreases, however, are only about 4.1 and 6.9% for 72W and 73W, respectively. The standard errors associated with the coefficients representing the slopes are similar in magnitude implying low significance of the slope changes. The resulting temperature shifts using averaged slope values are about 84 and 100°C for 72W and 73W, respectively. Using only the temperature intervals between the means and lower curves (representing one standard deviation on fracture toughness) results in associated standard deviations of 37 and 30°C for 72W and 73W, respectively, compared to 20°C and 22°C, respectively, for the CVN results.

Considering the combined data sets, with temperature normalized to ASME reference temperature, RT_{NDT}, the curve for the irradiated data is displaced upward in temperature because the fracture toughness shifts are greater than the CVN 41-J shifts. At K_{cl} values of 50, 100, and

200 MPa√m, the differences are about 10, 15, and 17°C. The standard deviation associated with the difference at 100 MPa√m is 13.7°C, a large value relative to the difference observed. The increasing temperature offset between the two curves with increasing K_{cl} reflects the average change in curve shape. The difference between the normalized unirradiated and irradiated curves for the combined data increases about 7°C over the K_{cl} range from 50 to 200 MPa√m, while the corresponding changes for 72W and 73W are 5.3 and 8.6°C, respectively, indicating a greater change in slope for the higher copper weld. Similarly, the corresponding change between the ASME K_{Ia} and K_{Ic} curves is 12.1°C. It is interesting that simple manual construction of bounding curves to the data result in measured temperature shifts within a few degrees of those determined by the various mean fits. Also, manually constructed curves, especially for 73W, suggest a shape change for the lower-bound curves.

Figure 2 shows a plot of the irradiated fracture toughness data and various curves for 73W. The ASME K_{Ic} curve is shown for the unirradiated condition and for the irradiated

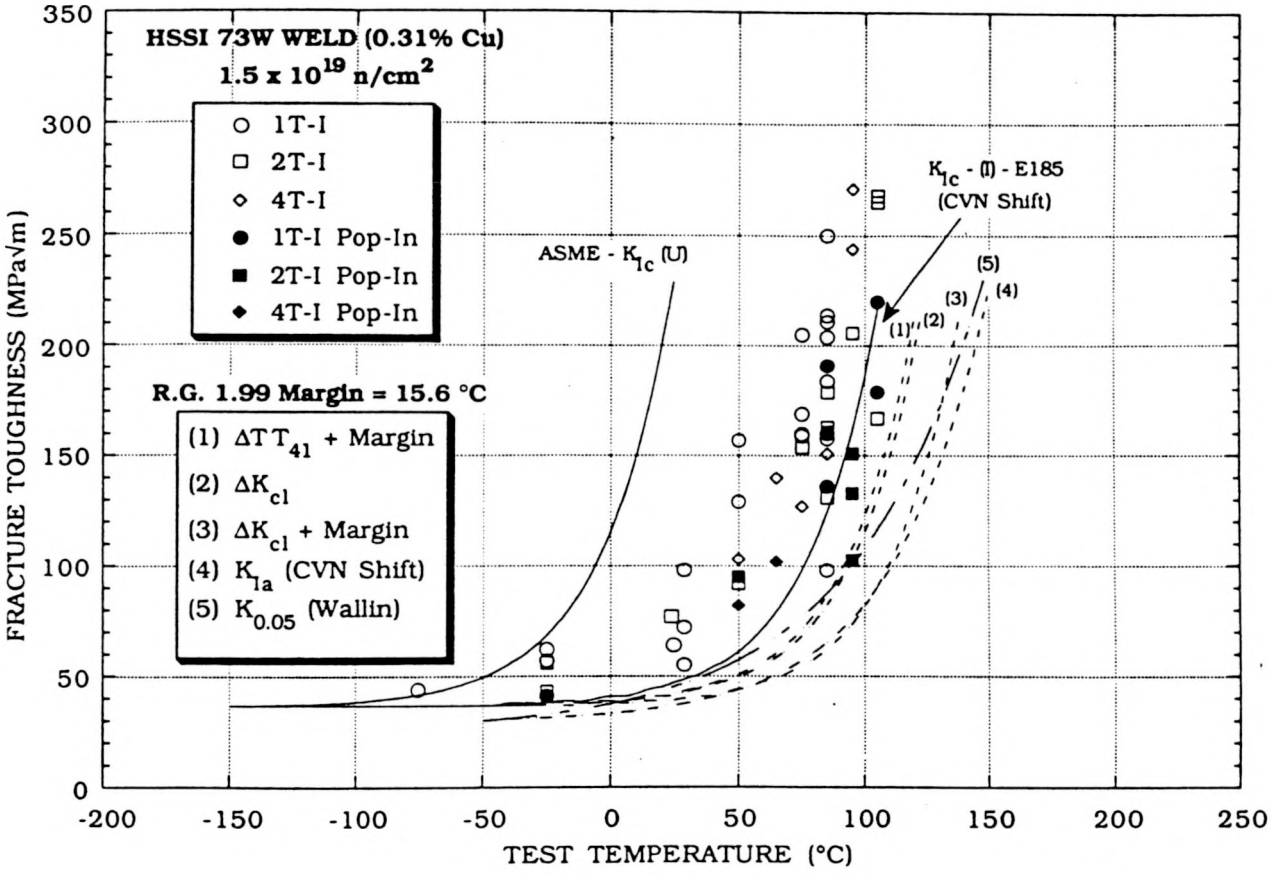

Fig. 2. Fracture toughness, K_{cl}, vs test temperature for irradiated HSSI weld 73W. The ASME K_{Ic} curve for the unirradiated data is shown as is the same curve after shifting it upward in temperature equal to the Charpy 41-J shift. The curves labeled 1, 2, and 3 represent the ASME curve shifted by the indicated criterion, where Margin is 15.6°C. The K_{Ia} curve represents the ASME K_{Ia} curve shifted by the Charpy 41-J shift. The $K_{.05}$ curve is the five-percentile curve for all the HSSI 72W and 73W combined data using the Wallin procedure.

condition after shifting the curve upward. The dashed curves labeled 1 through 3 represent different methods for shifting the K_{Ic} curve. The curve labeled 4 represents the ASME K_{Ia} curve shifted upward in temperature equal to the Charpy 41-J shift (ΔTT_{41}). The curve labeled 5 is the five-percentile curve produced using the method of Wallin.[4] For 72W, the data are bounded by the ΔTT_{41} + Margin curve and the ΔK_{cl} curve, but neither of those curves quite bound all the data for 73W. The margin is 15.6°C as defined in *Regulatory Guide 1.99* (Rev. 2) assuming credible surveillance data. The K_{Ia} curve is shown to allow for comparison of that curve with the shifted K_{Ic} curves, especially regarding curve shape in view of the observation that the irradiated K_{cl} curves for these two welds appear to have exhibited some shape change after irradiation.

Figure 3 shows a plot of all the irradiated fracture toughness data for 72W and 73W plotted vs temperature normalized to the RT_{NDT}. The RT_{NDT} for each weld is defined as the unirradiated RT_{NDT} plus ΔTT_{41}. As shown in the figure, a total of eight data points fall below the ASME K_{Ic} curve. The dashed curve is the K_{Ic} curve shifted upward in temperature to bound the data; a shift of 18°C is required.

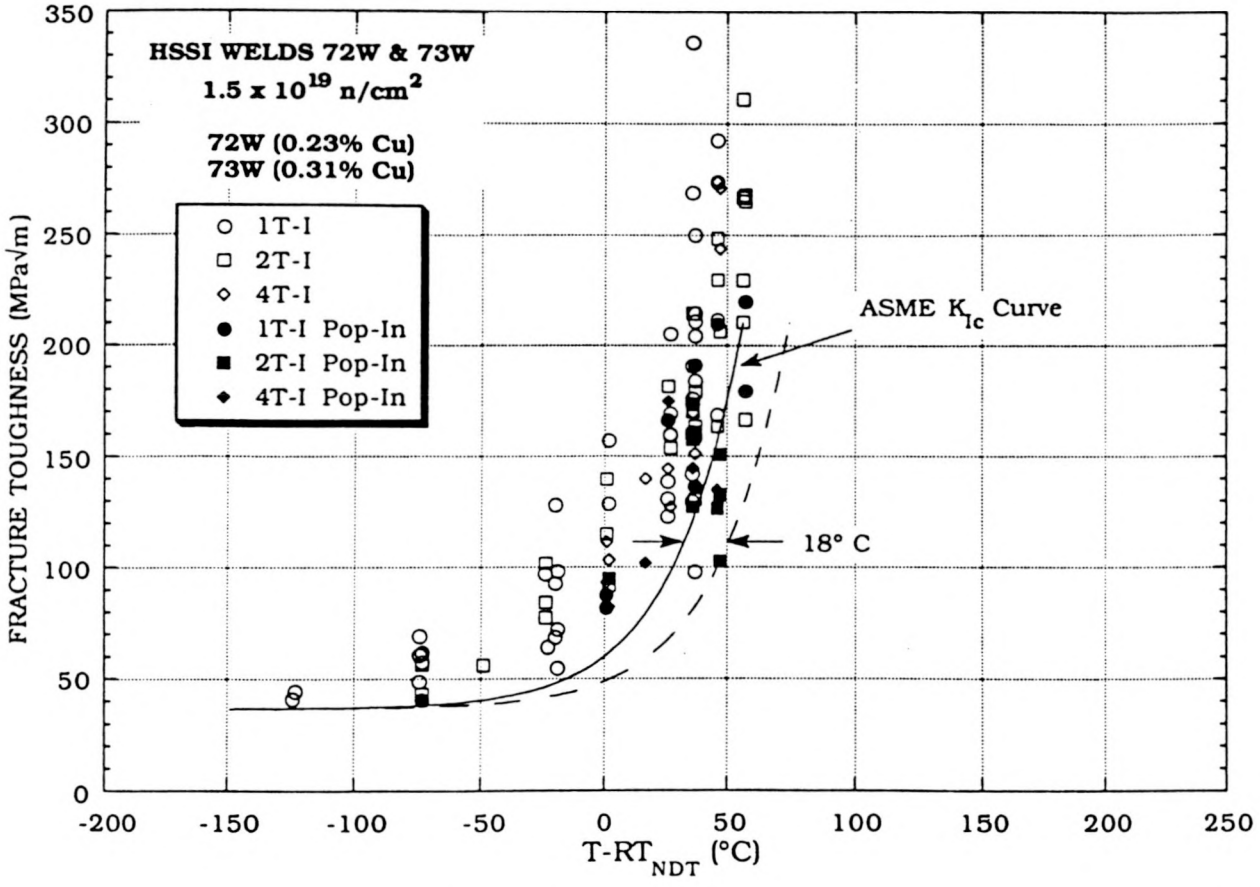

Fig. 3. Fracture toughness, K_{cl}, vs normalized temperature, T - RT_{NDT}, for the irradiated welds 72W and 73W. The dashed curve is simply the ASME curve shifted upward in temperature to just bound the irradiated data. As shown, an additional shift of 18°C beyond that of the Charpy 41-J shift is required.

Principal observations from the HSSI Fifth Irradiation Series are as follows. The fracture toughness values from small cleavage pop-ins suggest that the pop-ins observed in this study are significant relative to indicating propensity for cleavage fracture in the test specimen. Regarding the irradiation-induced temperature shift, statistical analyses and curve fitting showed that the temperature shifts at a fracture toughness of 100 MPa$\sqrt{m}$ were greater than those at a Charpy energy of 41 J, but are in good agreement with the Charpy 68-J transition shifts. The fact that the 68-J temperature shifts are greater than the 41-J shifts reflects the change in the slope of the CVN curves following irradiation.

Regarding the shape of the fracture toughness curve, the results from curve-fitting data are somewhat mixed. The linearized two-parameter fits, however, do indicate some decrease in the slopes, with the higher copper 73W weld exhibiting a somewhat greater change than for 72W. Using a 95% confidence criterion, however, those decreases in slopes are not statistically significant. On the other hand, curves constructed to bound all the data do indicate a substantial slope decrease, especially for weld 73W. Because the ASME K_{Ic} curve is a lower-bound curve for the data used for its construction, this latter observation is important. The five-percentile curve from the Wallin procedure bounds all the data, but the curve has a substantially lower slope than the ASME K_{Ic} curve and appears to be overly conservative at fracture toughness levels above about 100 MPa$\sqrt{m}$. Of course, concerns about curve shape changes can be accounted for by applying large enough shifts to the K_{Ic} curve, but such a practice begs the issue of the degree of accuracy that can be developed when the trend line (curve shape) does not fit the real fracture toughness trend for the irradiated condition. The data in the present case indicate that the K_{Ic} curve shifted by the 41-J Charpy V-notch plus margin would not have bounded a larger data base, and more margin adjustment is needed. The difficulty is that added margin to cover high toughness K_{cl} values will result in over-conservatism in the lower transition region. Therefore, shallower curves such as the five-percentile curve of Wallin or the K_{Ia} curve deserve consideration.

Preliminary observations from the HSSI Sixth Irradiation Series on crack-arrest toughness, described in the following section, indicate no irradiation-induced curve shape changes in the K_{Ia} curve.[5] One consideration, then, would be to use the K_{Ia} curve shape to describe the irradiated K_{Ic} curve for materials which exhibit irradiation-induced toughness shifts above some prescribed amount. The procedure used to construct the K_a curves was simply to translate the ASME K_{Ia} curve until it just provided a bound to the irradiated data. That procedure showed that, given the available crack-arrest data, the curves needed to bound the unirradiated and irradiated data are shifted from the ASME curve by less than ΔTT_{41}. For the combined irradiated data, the bounding curve is about 28°C lower than the shifted ASME K_{Ia} curve. Figure 4 shows a comparison of the ASME K_{Ic} and K_{Ia} curves as well as the bounding curves for the combined irradiated data for 72W and 73W normalized to the RT_{NDT} as discussed for Fig. 3. The most notable observation is that the K_{cl} curve has been shifted to higher temperatures than the K_a curve. An argument can be made that, because irradiation hardening increases yield strength, the strain-rate sensitivity is reduced such that the quasistatic K_{Ic} values tend toward agreement with the dynamic K_{Id} and K_{Ia} values. This does not, of course, account for the transposition of the K_{cl} and K_a results shown in Fig. 4. One important factor is the number of tests performed; 110 irradiated fracture toughness results and only 34 irradiated crack-arrest results are available. Further, the fracture toughness and crack-arrest toughness data for the unirradiated welds are not nearly as far apart as the ASME curves. By not considering the pop-ins in the irradiated fracture toughness data, the K_{cl} and K_a bounding curves would be very close. On the other hand, because the propensity for crack arrest increases with decreasing

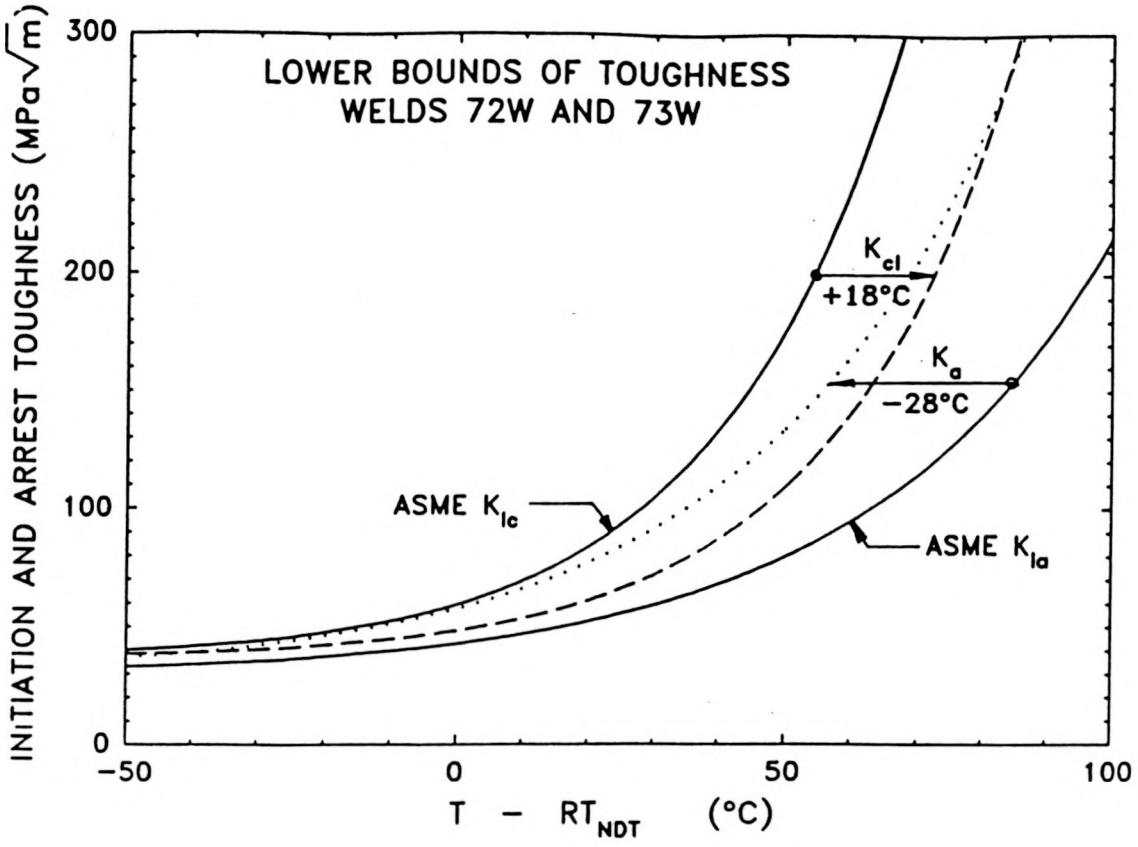

Fig. 4. Comparison of bounding curves for fracture toughness, K_{cl}, and crack-arrest toughness, K_a, vs normalized temperature, $T - RT_{NDT}$, for the irradiated welds 72W and 73W. The ASME K_{Ic} and K_{Ia} curves are included and show that the bounding curve to the K_{cl} data (110 test results) falls at higher temperatures than that for the K_a data (34 test results).

temperature interval between the K_{Ic} and K_{Ia} curves, many of the pop-ins may otherwise have resulted in fully broken specimens. Resolution of the observations in Fig. 4 most likely resides in consideration of statistical variations.

K_{Ia} CURVE SHIFT IN HIGH-COPPER WELDS

The primary objective of the HSSI Sixth Irradiation Series (or, for brevity, the K_{Ia} program) is to determine the effect of irradiation on the shift and shape of the K_{Ia} vs $(T - RT_{NDT})$ curve. The irradiations were performed by ORNL at the ORR at a nominal temperature of 288°C to average fluences of about 1.9×10^{19} neutrons/cm^2 (>1 MeV). Portions of the identical welds examined in the Fifth Series, 72W and 73W, were also used for the crack-arrest program. All crack arrest tests were performed by ORNL. All the dropweight, tensile, and Charpy impact results from the Fifth Series are applicable except for small adjustments required due to the higher fluence experienced by the crack-arrest specimens.

A total of 60 crack arrest specimens ranging in thickness from 25 to 33 mm were irradiated. Unirradiated specimens up to 51 mm in thickness were examined. The irradiated specimens included 36 weld-embrittled and 24 duplex-type specimens. The 36 weld-embrittled specimens have been tested in Phase I of the K_{Ia} program, and a detailed report has been published.[5]

Principal observations from Phase I are as follows. The shifts of the lower bound curves for the 72W and 73W welds are approximately the same as the corresponding ΔTT_{41}. Figures 5 and 6 show the results for welds 72W and 73W, respectively. Moreover, the shape of the lower bound curves compared to those of the ASME K_{Ia} curve did not seem to have been altered by irradiation for the test temperature range covered by the tests.

The crack-arrest toughness (K_a) data for welds 72W and 73W, both unirradiated and irradiated, have been plotted as a function of $T - RT_{NDT}$ in Fig. 7. The number of results plotted for each type of material tested is given beside each symbol in the legend. This figure includes a total of 77 unirradiated and 34 irradiated data points, many of which overlap. This figure shows that the four sets of K_a data when indexed to their respective RT_{NDT}s form a reasonable trend. The RT_{NDT}s for the four materials are given in Table 1. As shown in Fig. 7, the ASME curve is a conservative estimate of all the crack-arrest toughness data from

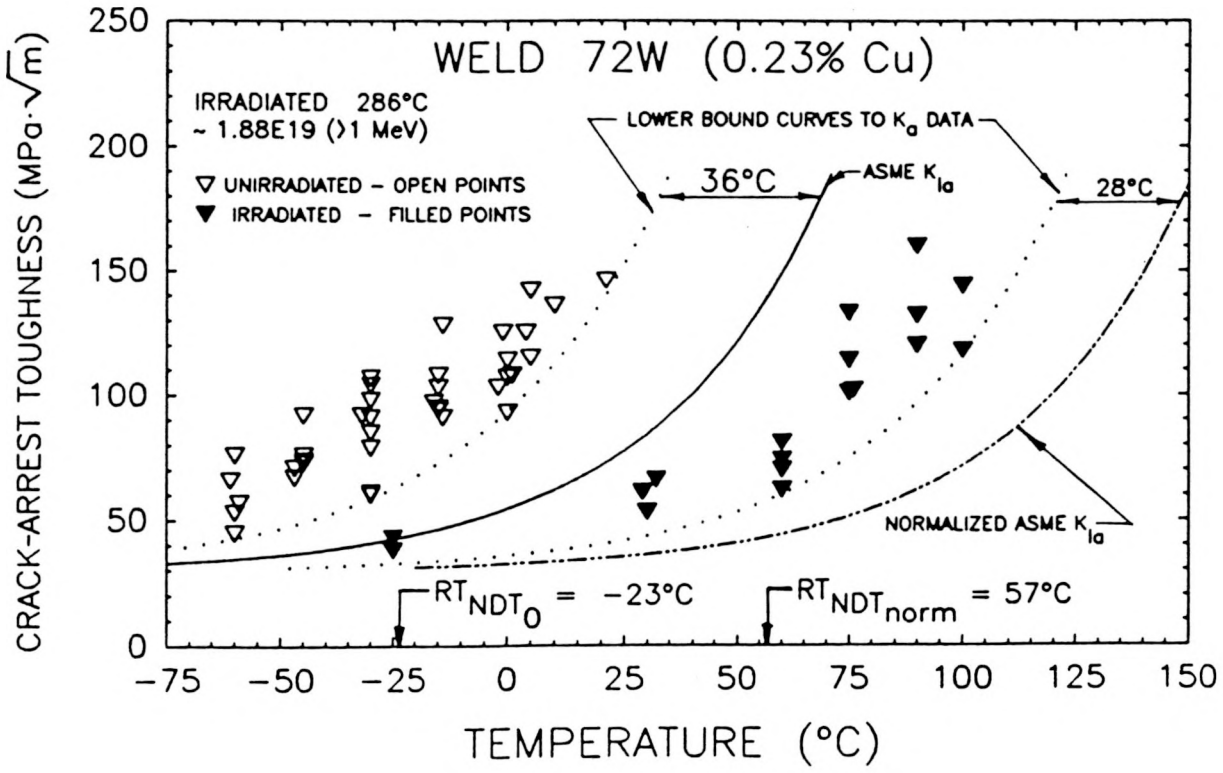

Fig. 5. Unirradiated and irradiated crack-arrest toughness, K_a, vs test temperature for weldment 72W. The dotted curves are lower bounds to the data obtained by shifting the ASME curves to a lower temperature by the amounts shown.

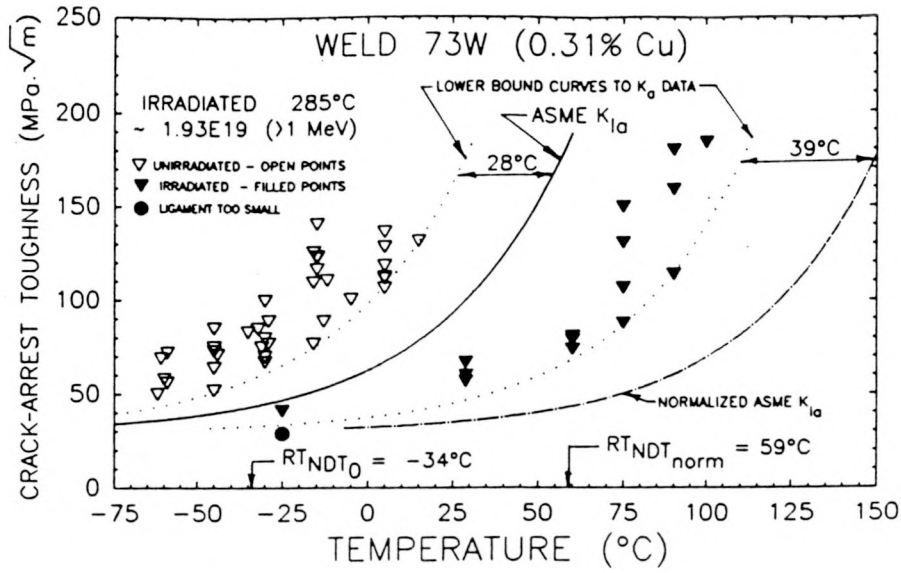

Fig. 6. Unirradiated and irradiated crack-arrest toughness, K_a, vs test temperature for weldment 73W. The dotted curves are lower bounds to the data obtained by shifting the ASME curves to a lower temperature by the amounts shown.

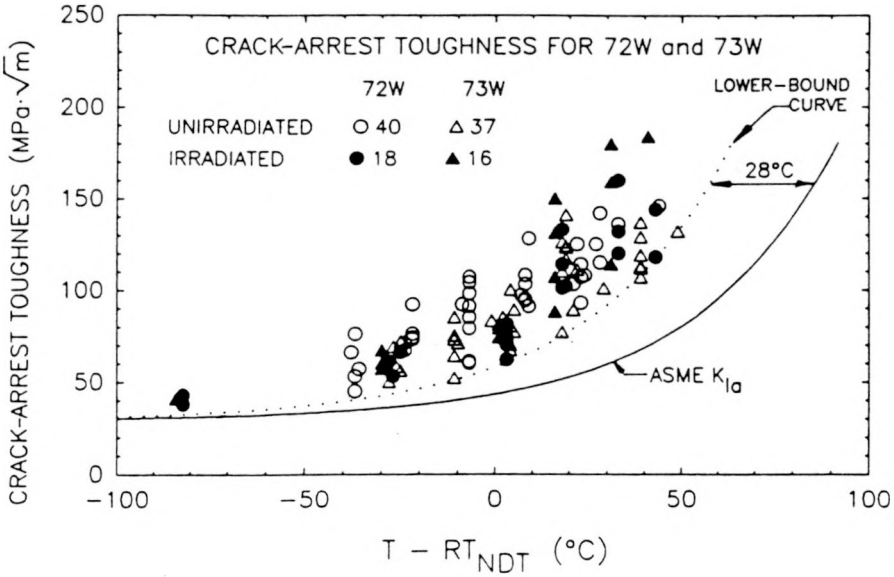

Fig. 7. All crack-arrest toughness K_a data for welds 72W and 73W plotted as a function of ($T - RT_{NDT}$). The number of results plotted are given beside each plot symbol in the legend.

Table 1. Initial, adjusted, and normalized reference temperatures (RT_{NDT}) for welds 72W and 73W

Weld	Initial RT_{NDT} (°C)	Charpy impact[a] observed results		Adjusted[b] RT_{NDT} (°C)	Charpy impact normalized[c] to crack-arrest fluences		Normalized RT_{NDT} (°C)
		Fluence, Φ (10^{19} n/cm^2) (>1 MeV)	ΔTT_{41} (°C)		Fluence, Φ' (10^{19} n/cm^2) (>1 MeV)	ΔTT_{41} (°C)	
72W	-23	1.51	72	49	1.88	80	57
73W	-34	1.51	82	48	1.93	93	59

[a]Source: R. K. Nanstad et al., "Effects of Radiation of K_{Ic} Curves for High-Copper Welds," pp. 214–33 in *Effects of Radiation on Materials: 14th International Symposium, Vol. II, ASTM STP 1046*, N. H. Packan, R. E. Stoller, and A. S. Kumar, Eds., American Society for Testing and Materials, Philadelphia, 1990.

[b]Adjusted RT_{NDT} = initial RT_{NDT} + ΔTT_{41} (according to ASTM 185–82).

[c]Normalization: $(\Delta TT_{41})(\Phi'/\Phi)^{0.5}$. Source: G. R. Odette and G. E. Lucas, "Irradiation Embrittlement of Reactor Pressure Vessel Steels: Mechanisms, Models, and Data Correlations," pp. 206–41 in *Radiation Embrittlement of Nuclear Pressure Vessel Steels: An International Review (Second Volume), ASTM STP 909*, L. E. Steele, Ed., American Society for Testing and Materials, Philadelphia, 1986.

NOTE:
Φ = fluence for Charpy V-notch impact specimens.
Φ' = fluence for crack-arrest specimens.
n = neutrons.
ΔTT_{41} = shift in 41-J Charpy V-notch impact energy level.

72W and 73W weldments in the transition region to approximately 50°C above RT_{NDT}. At temperatures below RT_{NDT}, there seems to be a smaller toughness margin between the lower-bound curves and the ASME K_{Ia} curves. For example, the lower-bound values are approximately 70, 35, and 10% higher than the ASME K_{Ia} values at temperatures with respect to RT_{NDT} of 50, 0, and -50°C.

The lower-bound curve, shown as a dotted curve in Fig. 7, is the ASME K_{Ia} curve shifted downward by 28°C in temperature until the first data point is encountered. The 28°C shift shown is the minimum shift from all four sets of data (unirradiated and irradiated welds 72W and 73W). The 28°C shift was obtained for the irradiated 72W weld and the unirradiated 73W weld and, thus, no trend can be established. However, it is quite possible that more experimental data may alter this lower bound significantly. The evaluation of the 72W and 73W crack-arrest toughness data obtained from the weld-embrittled specimens is ongoing. Statistical analyses, similar to those described in the previous section on the K_{Ic} program, will also be performed on the data.

The remaining 24 irradiated crack-arrest specimens, which are all duplex-type specimens, are being tested during Phase II of Series 6. Four of the 24 duplex-type specimens, two each from the 72W and 73W welds, have already been tested. In all four specimens the flaw arrested

in the fusion zone between the hardened crack-starter material and the weld metal test section. Porosity and lack of fusion were the major reasons for the crack arresting in that region. That is likely to preclude successful testing of the remaining duplex specimens in their present form. In order to utilize these specimens, various modifications to the duplex specimens are being considered. The initial modification being pursued is to increase the crack-driving force by increasing the diameter of the crack-starter hole. At present, the diameter of the hole in the 24 irradiated duplex specimens is approximately 4 mm. The idea behind this modification is that a sufficiently large increase in crack-driving force may cause the propagating flaw to jump across the unfused, porous zone, but still allow arrest within the test section of the specimen.

IRRADIATION EFFECTS ON STAINLESS STEEL CLADDING

The objective of the HSSI Seventh Irradiation Series is to obtain toughness properties for two types of stainless steel cladding in the unirradiated and irradiated conditions. The properties obtained include tensile, CVN impact, and J-integral toughness. The goal is to evaluate the fracture resistance of irradiated weld metal cladding representative of that used in early pressurized-water reactors. Irradiation effects on the single-wire, submerged-arc cladding have been published previously,[6] as have the irradiation effects on the tensile and Charpy impact behavior of three-wire cladding.[7] This section will summarize recently completed testing of irradiation effects on the fracture toughness of three-wire series-arc cladding.

The commercially produced three-wire series-arc stainless steel cladding was evaluated under similar irradiation and testing conditions as had been used previously for the single-wire cladding. To summarize results of CVN testing of the three-wire cladding specimens, irradiated at 288°C to fluence levels of 2 and 5×10^{19} neutrons/cm^2 (>1 MeV), it was observed that the CVN upper-shelf energy decreased by 15 and 20% and the 41-J transition temperature increased by 13 and 28°C, respectively. Irradiation also degraded the CVN lateral expansion significantly; expansion on the upper shelf was reduced by approximately 40% for both fluence levels. These results generally agree with those for the single-wire cladding produced with good welding practice.

Figure 8 shows that irradiation at 288°C to an average fluence of 2.41×10^{19} neutrons/cm^2 (>1 MeV) resulted in decreases in initiation ductile fracture toughness, J_{Ic}. Decreases in the tearing modulus were observed as well but the tearing modulus values did not change significantly with test temperature from about room temperature to 288°C. The J_{Ic} decreases generally agree with the reductions in both the CVN upper-shelf energy and lateral expansion except that the CVN data do not show a significant change with increasing test temperature.

Figure 9 provides a graphical comparison of the J_{Ic} values vs test temperature for the three-wire cladding with a typical A533 grade B class 1 plate (HSST Plate 02, 0.14 wt % copper) and a low upper-shelf weld (HSSI Weld 61W, 0.28 wt % copper), all in the unirradiated condition. Figure 10 shows a similar comparison of the same materials following irradiation at 288°C to similar fluence levels. Weld 61W gave the lowest J_{Ic} value (43.1 kJ/m^2) observed for the LUS welds tested in the HSSI Second and Third Irradiation Series.[9] The J_{Ic} of the irradiated cladding at 288°C is only about half that of 61W. It is also substantially lower than the lowest J_{Ic} value (83.3 kJ/m^2) obtained for HSST Plate 02 in the HSSI Fourth Irradiation Series.[10] The low fracture toughness of the three-wire stainless steel cladding has the potential for strongly affecting the extension of small surface flaws during overcooling transients.

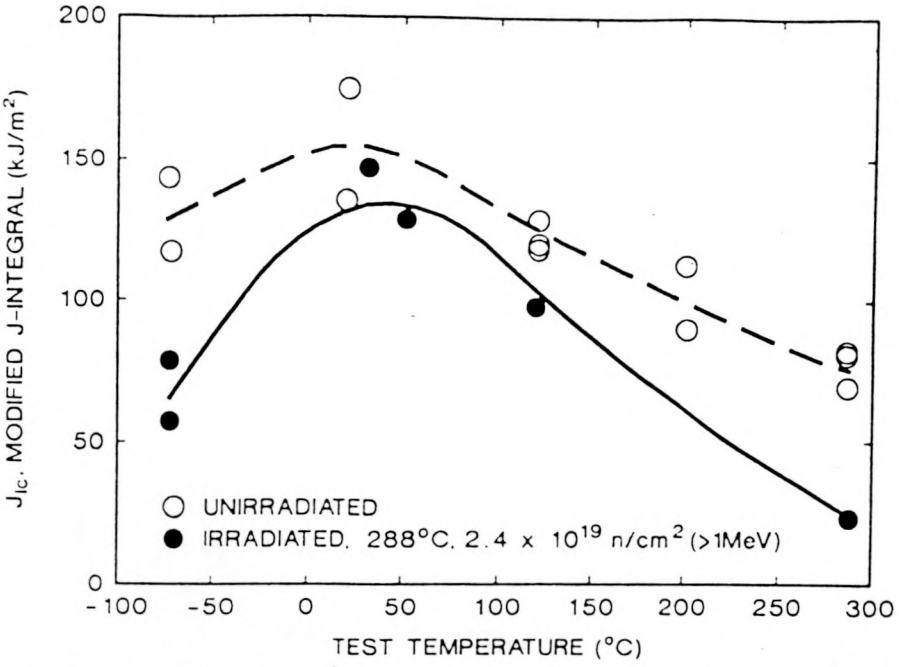

Fig. 8. Effect of irradiation on J_{Ic} initiation fracture toughness (modified J-integral) for type 308 stainless steel weld overlay cladding.

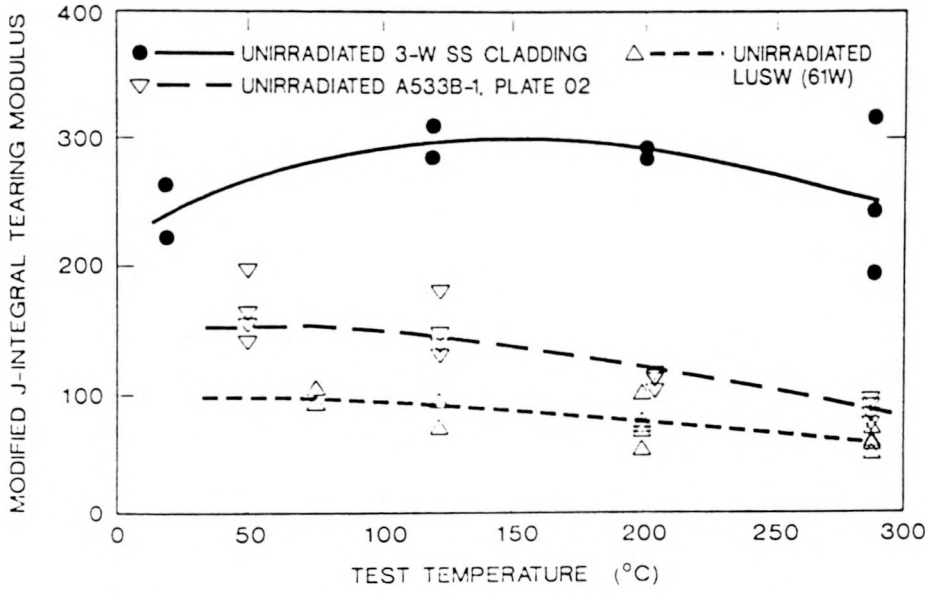

Fig. 9. Comparison between unirradiated J_{Ic} initiation fracture toughness (modified J-integral) for three materials, three-wire stainless steel cladding, low-upper shelf weld, and A533 grade B class 1 plate.

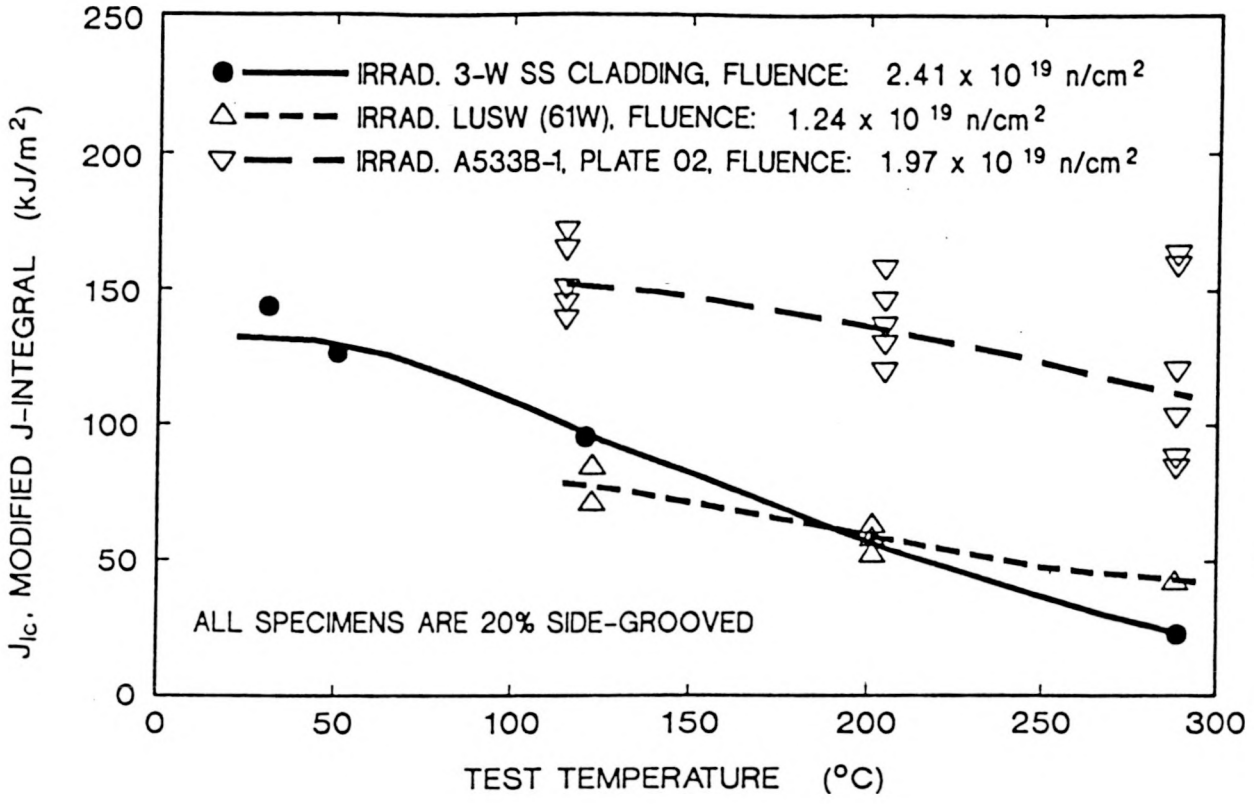

Fig. 10. Comparison between irradiated J_{Ic} initiation fracture toughness (modified J-integral) for three materials, three-wire stainless steel cladding, low-upper shelf weld, and A533 grade B class 1 plate.

A task to evaluate the effects of thermal aging on cladding is under way within the HSST program and some of the results from that task are directly germane to the HSSI Program. Short-term thermal aging of three-wire stainless steel weld-overlay cladding was conducted at 288°C for 1605 h, the same temperature and exposure time corresponding to the irradiation of this material to a fluence of 5×10^{19} neutrons/cm^2 (>1 MeV). The Charpy upper-shelf energy showed a decrease of 16%, comparable to the 22% decrease from the combined effects of aging and irradiation. The 41-J transition temperature shift was only 3°C compared to the 29°C shift observed in the irradiation experiment. Finally, thermal aging caused only a very small change in the tensile properties compared to yield strength increases varying from 6 to 34% (dependent on test temperature) due to the irradiation exposure. Effects of short-term thermal aging on dynamic and static fracture toughness is being examined and will be reported later. Furthermore, long-term aging experiments are under way at 288°C for 20,000 and 50,000 h, and at 343°C for 20,000 h.

K_{Ic} AND K_{Ia} CURVE SHIFTS AND ANNEALING IN LOW UPPER-SHELF WELDS

This task focuses on examining the fracture behavior of irradiated and post-irradiated and annealed welds with low resistance to ductile tearing. It will provide, if needed, a basis for

modification of the current method for shifting the various ASME fracture toughness curves (K_{Ic}, K_{Ia}, K_{IR}) to account for irradiation embrittlement, specifically in LUS welds. The information developed under this task will augment that obtained in experiments performed on two high upper-shelf weldments under the Fifth and Sixth Irradiation Series and provide an expanded basis for accounting for irradiation-induced embrittlement in reactor vessel materials. Additionally, it will examine the effects of thermal annealing and reirradiation on K_{Ic}, K_{Ia}, and ductile tearing resistance (J-R) in large specimens representative of reactor vessels. The planning for these irradiation experiments, designated Series 8 (K_{Ic} and K_{Ia} curve shifts) and Series 9 (annealing effects) has begun but procurement of material and irradiations will not start before 1992.

IRRADIATION EFFECTS IN COMMERCIAL LOW UPPER-SHELF WELDS

The focus in this task is the investigation of commercially produced submerged-arc welds with low Charpy upper-shelf energy. It will substantially augment the information obtained in the HSSI Second and Third Irradiation Series which examined the effects of irradiation on the ductile fracture toughness of commercially fabricated LUS welds. All of these welds have been fabricated with Linde 80 flux and copper-coated weld wire. The task currently includes two subtasks, the investigation of welds from the Midland Reactor Vessel, and the final analyses of irradiation temperature and fluence variations on the tensile and Charpy impact data from the Second and Third Series.

Irradiation Effects in the Midland Reactor Vessel Weld

The primary objective of the HSSI Tenth Irradiation Series is to investigate the postirradiation fracture toughness of the WF-70 submerged-arc weld from the Midland Unit 1 reactor vessel. The weld metal is known to be low upper-shelf energy material, and this same weld material (WF-70) is known to be the controlling material in five commercial operating reactors. The test program will provide vital information on the significance of test methods that are applied in surveillance programs.

Consumers Power Company canceled and legally abandoned the facilities at Unit 1 of the Midland Power Station. The reactor vessel of Unit 1 was fabricated with a complete circumferential seam weld of WF-70 material at the core beltline. The WF-70 designation by Babcock and Wilcox, Co. (B&W) is the identification of a particular heat of weld wire (72105) and particular lot of Linde 80 welding flux (8669). The circumferential double-butt nozzle weld seam, interrupted by the nozzles, was fabricated using WF-70 on the outer half and WF-67 on the inner half of the weldment. Procedure WF-67 used the same Linde 80 welding flux as for WF-70, but used a different heat of weld wire (72442). Consumers Power Company provided the material free of charge as an act of goodwill for the benefit of the nuclear industry. A joint effort was initiated, at the instigation of the USNRC and the Electric Power Research Institute (EPRI), to obtain the WF-70 welds from the Unit 1 reactor vessel. Participants in the effort included Commonwealth Edison, B&W Owners Group, Westinghouse Electric Owners Group, and ORNL (representing the USNRC). Blocks of material, about 1.2 m long and 0.7 m wide, were removed from the 216-mm-thick vessel beltline region and the 305-mm-thick nozzle region by air-arc gouging the stainless steel cladding and flame cutting the base material using a vacuum-mounted fixture. Five beltline and two nozzle course sections were obtained by ORNL.

A plan for evaluating the WF-70 welds has been completed and includes both unirradiated and irradiated testing. In addition to a detailed characterization of the bulk chemical composition

of the welds, the field-ion microscope-atom probe will be used to determine the matrix composition of certain elements, e.g., copper, thought to better represent the amount of those elements available to the radiation damage process. Charpy and drop-weight tests have been performed at various locations through the weld thickness as well as at various locations along the weld to examine the variability in the unirradiated RT_{NDT}. Charpy, tensile, drop-weight, and compact specimens of various sizes will be tested in the irradiated and unirradiated conditions. In the transition region, 0.5T, 1T, 2T, and 4TC(T) specimens will be tested in the unirradiated condition, while 0.5T, and 1TC(T) will be tested in the irradiated condition. On the ductile shelf, J-integral resistance curves will be obtained using compact specimens from 0.5T to 4T unirradiated and up to 2T irradiated, with the possibility that 4TC(T) specimens would be irradiated if the unirradiated J-R tests show significant size effects. The J-R behavior of the WF-70 weld metal is of great interest, especially regarding potential size effects on the tearing modulus. In addition a limited number of crack-arrest specimens will be irradiated and tested.

The first of two levels of testing is the preliminary evaluation of the material for uniformity of properties. Four beltline weld sections that cover the full 360° have been sampled and the testing is complete except for chemical analyses on two of the sections. The nozzle course weld sections have been sampled but the testing is not yet completed. Table 2 summarizes the transition temperature indices for the four beltline sections. Only the 1/4 thickness (1/4t) position of section 15 appeared to show significantly different 41- and 68-J temperatures as a function of depth in the weld. Nil-ductility temperatures appear to be consistent also. The variation in 41-J transition temperature throughout the weld, however, is from -19 to +15°C. In all cases, the RT_{NDT}s are determined by the CVN data. The upper-shelf energies vary from 66 to 107 J; the 3/4t location in section 15 is the only sampled location which resulted in an upper-shelf below the 68-J (50 ft-lb) limit permitted by the USNRC.

Table 2. Transition temperatures for Midland beltline welds, codes 13, 9, 11, and 15

Through-thickness position	Charpy V-notch tests												NDT temperature (°C) at code number			
	41-J temperature (°C) at code number				68-J temperature (°C) at code number				Upper-shelf energy (J) at code number							
	13	9	11	15	13	9	11	15	13	9	11	15	13	9	11	15
1/4t	-13	-6	-7	4.1	22	34	26	53	102	76	90	84	-60	-60	-60	-45
1/2t	-17	-11	-2	-13	29	25	21	23	105	83	90	90				
5/8t	-19	-15			10	14			107	87	90	90				
3/4t	0	3	15	12	36	53	53	[a]	89	81	83	66	-45	-45	-50	-55
7/8t		-3	-14	-10		44	31	27		78	79	84				

[a]Material did not attain 68-J energy level.

Test results of K_{Jc} fracture toughness with compact specimens are shown in Fig. 11. The beltline specimens came from 1/4t and 3/4t positions, while nozzle course specimens came only from the 3/4t position. Variable conditions of side-grooved vs not side-grooved and through-thickness position did not show significant trends.

Chemical analyses have been performed on two beltline and two nozzle course sections with a full analysis at five locations through the thickness in each case. The chemical

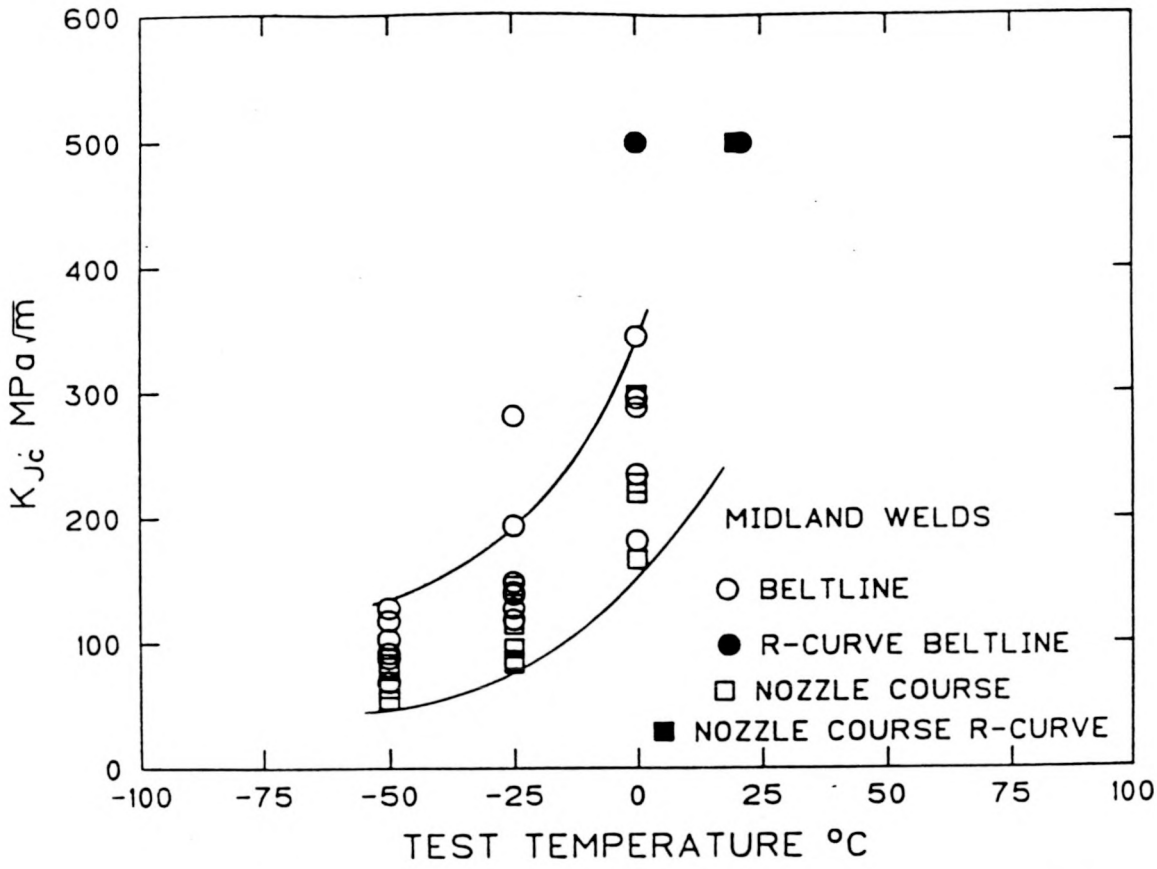

Fig. 11. K_{JC} data from the Midland WF-70 welds at four locations around the beltline and two locations around the nozzle course.

compositions are generally as expected except that the copper content in the beltline sections is significantly lower than that in the nozzle course sections. The copper content ranges from about 0.21 to 0.32% with an average value of about 0.26% in the beltline, while the nozzle sections show a range of 0.36 to 0.46 with an average value of about 0.41% for the WF-70 portion of the weld. The most likely cause of the large variation derives from the variability of the coating processes used to apply the copper coating to the weld wire. This observation required revision of the preliminary irradiation plan which was predicated on a Linde 80 weld with typical copper variation. Thus, the current irradiation plan has been modified to incorporate the investigation of two weld metals, one obtained from the high-copper WF-70 of the nozzle weld and the other from the lower copper beltline weld.

Evaluation of the degradation of properties due to irradiation damage will begin following the completion of the initial study of chemistry and fracture property distributions. Both high and low copper-content weldmetals will be examined at three levels of irradiation, 5×10^{18}, 1×10^{19}, and 5×10^{19} neutrons/cm^2 (>1 MeV). The lowest and highest fluences would be investigated only with CVN, tensile, and 0.5TC(T) specimens. The bulk of the irradiations would be conducted at 1×10^{19} and would include at least two large capsules with the specimen complement stated earlier. Sufficient specimens will be irradiated and tested to investigate

material variability. One area of emphasis will be a comparison of transition temperature shifts from surveillance capsule size specimens vs those from the larger specimens. The latter are more likely to agree with ASME Code curve behavior. R-curve trends for upper-shelf behavior will also be evaluated in terms of surveillance specimens vs the larger specimens that will yield more J values (as per ASTM E 1152) for J_R curve development. Design of the large capsules is presently underway with irradiations scheduled to begin during 1991 at the Ford Nuclear Reactor at the University of Michigan.

Analyses of Charpy and Tensile Data From Irradiation Series 2 and 3

The HSSI Second and Third Irradiation Series had the primary objective to investigate the effects of irradiation on the ductile fracture of seven commercially fabricated LUS submerged-arc welds. All the welds were fabricated with copper-coated wire and Linde 80 flux which produced welds with relatively low Charpy upper-shelf energy in the unirradiated condition and of relatively high sensitivity to neutron radiation. The development of experimental elastic-plastic fracture mechanics methods was pursued concurrently with the conduct of these irradiation series. The irradiation of compact specimens up to 4TC(T) and testing of those specimens to obtain J-integral resistance curves represented a major undertaking which was shared by a number of organizations.

Irradiation of the compact specimens at a nominal temperature of 288°C to an average fluence of about 8×10^{18} neutrons/cm^2 (>1 MeV) was relatively successful and their results have been published previously.[9] However, the Charpy impact and tensile specimens were located at positions in the capsule where temperature control was less and the irradiation temperatures spanned the range 235 to 345°C for those specimens. Additionally, the neutron fluences for the small specimens varied from about 4 to 13×10^{18} neutrons/cm^2 (>1 MeV). Although not desirable within the intended context of the experiments, those variations did provide the opportunity to investigate the effects of irradiation temperature and fluence (over the ranges observed) on the tensile and Charpy impact properties of these LUS welds. The data available for such analyses was limited from a statistical viewpoint, yet allowed for some reasonable observations which could be compared with results from other studies. For most of those comparisons, the Charpy and tensile results were normalized for fluence variations to the average fluence of 8×10^{18}. The results of the irradiations and their analyses have been recently published.[11] The important observations and conclusions which can be stated based on the results of those analyses are summarized here.

Analyses of irradiated tensile data showed a dependence on irradiation temperature of -1.15 MPa/°C for yield strength, -0.79 MPa/°C for ultimate strength, and -0.014%/°C for total elongation. Analyses of irradiated Charpy data showed a dependence on irradiation temperature of about -0.5°C/°C for transition temperature shift and -0.05 J/°C for upper-shelf energy drop.

The results indicated that the radiation-induced changes in yield strengths (in megapascals) and Charpy transition temperature shifts (in degrees Celsius) for the seven welds can be expressed as $\Delta TT_{41} = 0.70 * \Delta s_y$. The Charpy results indicated a dependence on copper concentration which can be expressed as $\Delta TT_{41} = 234 * (Cu - 0.1)^{0.57}$, where ΔTT_{41} is degrees Celsius and copper (Cu) is weight percent.

Comparison of the Charpy results with data for the same materials irradiated in power reactor surveillance programs showed mixed results with the power reactor changes being greater in some cases and the test reactor changes greater in others.

MICROSTRUCTURAL ANALYSIS AND MODELING

Over the past thirty years, a large amount of experimental data has been accumulated on the irradiation embrittlement of pressure vessel steels. Specimens irradiated in materials test reactors and surveillance locations of operating power reactors have been used to flesh out the irradiation property change response of these materials. However, in the broader context of research on radiation effects phenomena in materials, embrittlement historically has been treated in a qualitatively different manner. Other phenomena such as irradiation-induced swelling, creep, solute segregation, precipitation and helium-affected ductility loss have been subject to more mechanistically oriented work covering two areas. The first is extensive microstructural and microcompositional analysis using analytical electron microscopy (AEM) and other techniques. Irradiation response on the atomic and microstructural scales has been characterized with respect to both materials parameters and irradiation variables. The second is the development of fundamental understanding of the observed phenomena. The most detailed and quantitative expression of this understanding is in the formulation of physically-based theoretical models describing macroscopic property changes and their relation to the atomic and defect level structure.

The situation has changed recently concerning pressure vessel steels. Greatly increased capabilities are now available for atomic- and defect-scale characterization. It is now possible to reliably identify the irradiation-induced clusters responsible for hardening and to characterize them with respect to size, density, and elemental composition, for example. Modern capabilities can now be used to develop an understanding of embrittlement on a physical basis commensurate with the current knowledge in the other areas of radiation effects.

A physical theory based on defect reactions and microstructural evolution can now be formulated. It needs to be tethered soundly on the microstructural level by results from the microstructural characterization techniques, and constrained at the macroscopic level to produce predictions consistent with the large array of macroscopic embrittlement measurements. Models of this type formulated to describe swelling, irradiation creep, solute segregation and high temperature ductility loss have proven remarkably successful. A viable theoretical model will result in predictions of embrittlement for conditions where experimental data are unavailable (temperature, dose rate, dose) but where behavior must be known. It is expected to also provide guidance for the design of embrittlement-resistant alloys tailored for specific irradiation conditions. Results of the initial work within the HSSI program in this task are described below, focussing on two principal areas of effort. One is an analytical evaluation of embrittlement effects focusing on rate effects in general and the initial hardening transient in particular. The other is an experimental effort to obtain definitive information on spectrum and rate effects at low temperatures, similar to those at which vessel supports operate.

Transient and Rate Effect on Embrittlement

The reaction rate theory description of radiation damage has been widely used to model phenomena such as void swelling and irradiation creep. That work has generally been concerned with irradiation conditions of relatively high doses (>1 dpa) and high temperatures (T > 300°C). In that regime, the vacancies and interstitials rapidly come into equilibrium with the microstructure and it is safe to assume that the point defect concentrations are at their steady state values. Point defect behavior in the steady state has been thoroughly explored.[11-15] Analytical solutions to the rate equations have been obtained for certain limiting cases that describe the dependence of the point defect concentrations on the total dose or the displacement rate.[11-16]

In contrast, the time required for the point defect concentrations to reach steady state at the lower temperatures typical of reactor pressure vessels and reactor support structures can be quite long, at the lowest temperatures even exceeding the in-service component lifetime.[16] Therefore, the use of the steady-state point defect concentrations in models for the behavior of materials in this regime can give irrelevant and misleading results. A simple model has been developed and used to conduct a detailed numerical analysis of the influence of the point defect transient. This initial work has focused on the influence of the displacement rate because of the importance of accelerated testing to research on pressure vessel embrittlement. The number or fraction of point defects that are lost to bulk recombination have been used as a measure of radiation sensitivity, since it is only defects that escape recombination that are available to contribute to radiation-induced embrittlement.

The number of point defects that have recombined up to some time, t, can be calculated as

$$NR = \int_0^\tau RC_iC_v dt\,, \tag{1}$$

where R is the bulk recombination coefficient and C_i and C_v are the interstitial and vacancy concentrations, respectively. Using the limiting values of C_i and C_v that are obtained during the linear portion of the point defect transient and at steady state for sink-dominated point defect absorption,[12,16] analytical expressions for the number and fraction of point defects lost to recombination were derived. These expressions are listed in Table 3, where the dose, Δ, is the product of the modified displacement rate (G'_{dpa}) and the time, and the $D_{i,v}$ and $S_{i,v}$ are the diffusivities and total sink strengths for interstitials and vacancies.

Table 3. Number (N_R) and fraction (f_R) of point defects lost to recombination for limiting cases

	NR	fR
Linear transient	$\frac{R}{3}\frac{\Delta^3}{G'_{dpa}}$	$\frac{R}{3}\frac{\Delta^2}{G'_{dpa}}$
Steady state, recombination dominant	$\frac{RG'_{dpa}}{D_iD_vS_i^TS_v^T}\Delta$	$\frac{RG'_{dpa}}{D_iD_vS_i^TS_v^T}$

The symbol G'_{dpa} represents the generation rate of defects that avoid in-cascade recombination, i.e., the actual displacement rate times the fraction that avoids in-cascade recombination. The expressions listed in Table 3 provide an estimate for how the recombination fraction changes with the displacement rate. Alternately, the change in the irradiation time required to give equivalent recombination fractions at different displacement rates can be

calculated. The recombination fraction exhibits a quadratic dependence on the dose during the transient (low doses) and is independent of the dose at steady state (high doses). At a given dose, the recombination fraction is inversely proportional to the displacement rate during the transient and linearly dependent on the displacement rate at steady state.

The number of vacancies lost to recombination at doses between the limits discussed above was obtained by explicitly integrating the rate equations describing the time dependence of the point defect concentrations and using Eq. (1). The results obtained at 275°C for a range of displacement rates that include test reactor and LWR surveillance specimen conditions are shown in Fig. 12. For the value of the dislocation sink strength used here, 10^{11} cm^{-2}, point defect loss is sink-dominated for most of the curves shown in Fig. 12. This can be seen in Fig. 13 where the fraction of the radiation-produced vacancies lost to recombination is plotted in the same way for these same conditions. For displacement rates less than $\approx 10^{-8}$ dpa/s, the bulk recombination fraction is less than 10%. The recombination fraction increases with displacement rate because the interstitial and vacancy concentrations increase. While the number of point defects lost to sinks increases linearly with C_i or C_v, the number recombining in the bulk increases quadratically.[12,16]

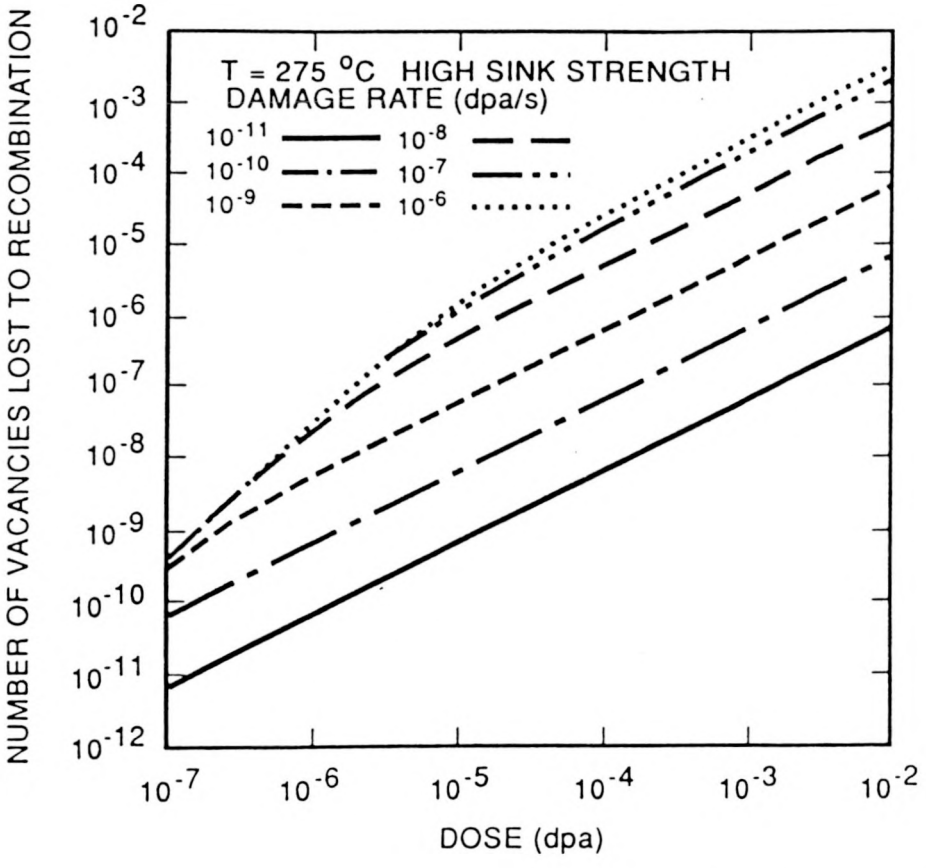

Fig. 12. Displacement rate dependence of the number of vacancies lost to recombination as a function of dose at 275°C. Dislocation sink strength is 10^{11} cm^{-2}.

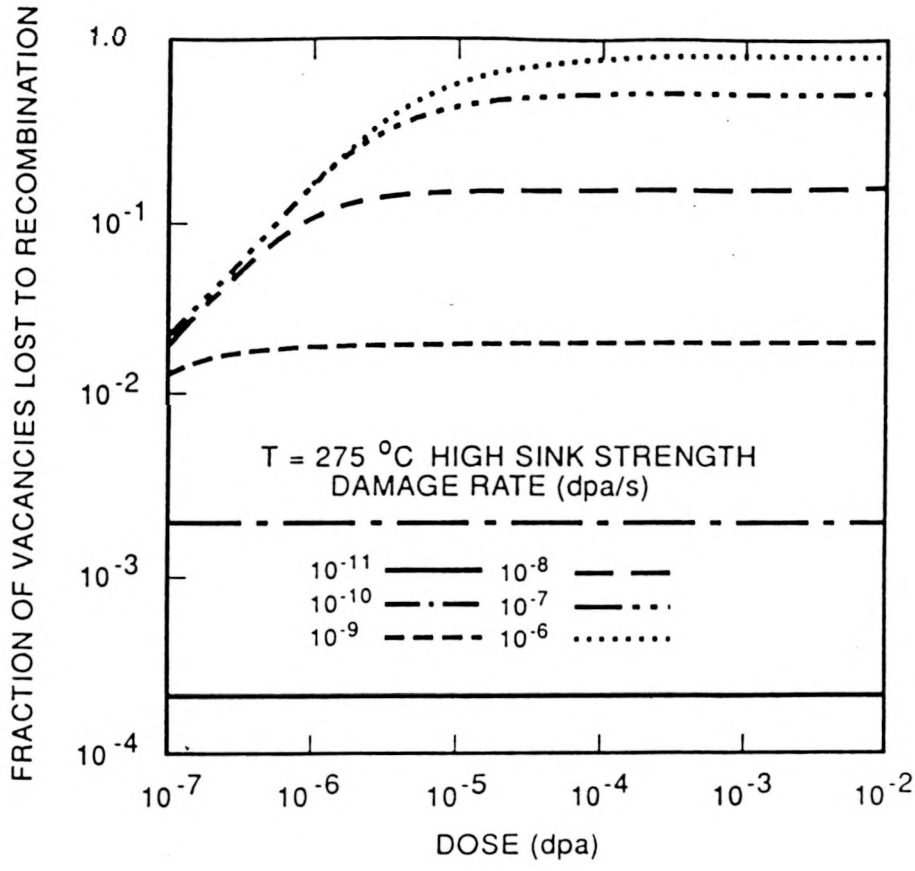

Fig. 13. Fraction of vacancies lost to recombination as a function of dose at 275°C. Same conditions as Fig. 12.

To illustrate the range of observed behavior, and to highlight the difference between transient and steady-state conditions, additional results at lower doses are shown in Fig. 14. Consistent with the calculated limiting behavior listed in Table 3, the number recombining exhibits a cubic dose dependence at low doses and a linear dependence at high doses. At low doses, the number recombining decreases as the displacement rate increases, but the dependence on displacement rate is reversed at high doses. The transition between "low-dose" and "high-dose" behavior occurs near the dose required for the vacancy concentration to reach steady state.

The time or dose required for the point defect concentrations to reach their steady state values is strongly dependent on the irradiation temperature and the sink structure. For temperatures below about 200°C, the extent of the point defect transient can be comparable to the component lifetime or to the duration of an irradiation experiment. Thus, theoretical analysis that relies on the assumption of steady state at these conditions is not valid. The results of the time-dependent analysis presented here show how the dose dependence of point defect absorption (measured as the complement of the recombination fraction) changes continuously between limiting values characteristic of the initial transient and the steady state. The displacement rate dependence of point defect absorption also varies between these limits and is a function of the sink structure.

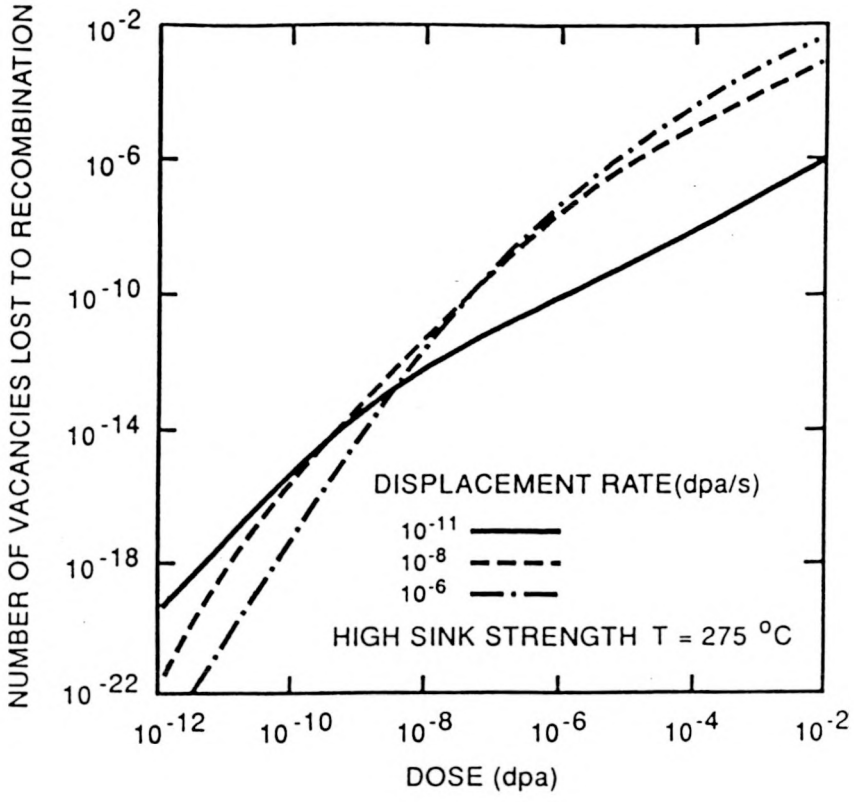

Fig. 14. Displacement rate dependence of the number of vacancies lost to recombination as a function of dose at 275°C for sink-dominant conditions. Similar to Fig. 12, but over a large dose range.

The use of test reactor irradiations to predict behavior at lower displacement rates must then consider these two confounding factors. First, the duty cycle of the test reactor can influence the analysis. For power reactor pressure vessels and other out-of-core components, where operating temperatures may be above 200°C, the point defect transient may be exceeded at a relatively small fraction of the component lifetime. But, in a test reactor at the same temperature, frequent start-ups and shut-downs may lead to the experiment being conducted entirely within the point defect transient. Secondly, since the effect of displacement rate is different in the transient and steady state regimes, data extrapolation from test reactor irradiations may cross mechanism boundaries and lead to poor estimates of material response at low displacement rates.

Neutron Spectrum and Flux Effects Experiments

The assessment of the premature embrittlement of the pressure vessel of the High Flux Isotope Reactor (HFIR) at ORNL[17] prompted an analysis of the effects of neutron spectrum on embrittlement of ferritic steels,[18,19] that indicated thermal neutrons as the likely cause of the early embrittlement. It was pointed out that embrittlement arises from self- and solute-clusters of irradiation-produced point defects. Only a small fraction of the total point defects produced by

atomic displacements are involved in the clusters. The bulk of the point defects are lost by recombination within the displacement cascades where they are created, so only the surviving point defects are relevant to embrittlement. Thermal neutrons make small cascades via (n,g) recoils, and the point defects made in such cascades have a much greater probability of survival than those born in the large dense cascades associated with fast neutrons. Therefore, thermal neutrons should create more surviving point defects per unit displaced atom than fast neutrons, perhaps a factor of ten more. Determining the magnitude of the weighting factor for the thermal neutrons is crucial. It means that for irradiations in a neutron spectrum where more than 10% of the atomic displacements are caused by thermal neutrons, the resulting damage to microstructure and mechanical properties should be dominated by thermal neutrons, not by fast neutrons as is traditionally supposed. If damage is assessed solely in terms of fast neutrons, which is the conventional way, the contribution from thermal neutrons will be considered negligible or minor, and embrittlement in a highly thermalized neutron spectrum will appear to be accelerated.

At the HFIR vessel, preliminary calculations indicate that the spectrum contains upwards of 96% thermal neutrons, which implies that more than 30% of the atomic displacements are created by thermal neutrons. But the neutron fluxes there are too low to permit confirmatory embrittlement experiments to be made in reasonable times. Therefore, to substantiate the hypothesis regarding spectrum effects experiments were initiated in the heavy-water High Flux Beam Reactor (HFBR) at Brookhaven National Laboratory. One scoping run was made before the reactor was shutdown in response to a safety question. When it became apparent that the HFBR would be down for a protracted period, it also became apparent another reactor with a high flux, highly-thermalized spectrum would be required.

The hydraulic facility of the NRU reactor at Chalk River, Canada was selected with Chalk River to provide neutron exposures and mechanical testing and ORNL to provide specimens, encapsulation and neutron dosimetry. Irradiation capsule designs have been approved and a thorough dosimetry survey of two sites in the hydraulic facility has been completed. The neutron conditions in the facility are ideal for the experiments. The neutron fluxes ($>10^{12}$ fast neutrons/cm^2-s and $>10^{14}$ thermal neutrons/cm^2-s) are high enough to induce embrittlement in exposure times of a few weeks, and the spectrum is more than 95% thermal neutrons.

The experiments have two goals. One is to obtain embrittlement data in a soft spectrum to compare with existing data for a harder spectrum. The other is to measure the contribution of thermal neutrons to embrittlement by using cadmium wrappers around the specimens to absorb the thermal neutrons. Specimens will be irradiated over a range of fluences, with and without cadmium wrappers, and the changes in tensile yield stress will be measured as an index of embrittlement. The test materials consist of four different ferritic steels. Two of these, A212B and A350, are HFIR pressure vessel archive materials for which there is reference tensile embrittlement data obtained after irradiations in the HFIR and the ORR. A third steel is A36, which is of interest for external reactor support structures. The fourth is A533B, pertinent to commercial light water reactor vessels. Irradiation of the specimens is scheduled for late in 1991.

To fully explore the possibilities which may influence irradiation effects on pressure vessel support materials, which experience a temperature and neutron exposure rate in some ways similar to that of the HFIR vessel,[17] experiments were begun to examine potential neutron flux effects under realistic exposure conditions for vessels supports. To compliment the experiments in the Chalk River reactor designed to explore the potential for a spectrum-induced acceleration during low temperature irradiation embrittlement, specimens are being exposed in the cavity surrounding the RPV in the Trojan pressurized water reactor. It is anticipated that these specimens will be exposed to a neutron fluence of roughly 2×10^{17} neutrons/cm^2 (E > 1MeV)

over a period of about two years. This will produce a fast neutron exposure of a level comparable to that seen in the HFIR vessel, at a flux of only one order of magnitude higher. In addition the spectrum, which is being extensively characterized for the HSST program, will be typical of at least one possible set of conditions which exist in a reactor cavity and could be experienced by vessel support materials. By comparing the results from this effort with the those from the HFIR surveillance program and those from the Chalk River reactor exposure, it should be possible to gain a substantially enhanced knowledge of the causes of the accelerated embrittlement observed in the HFIR vessel and its application to reactor pressure supports.

Specimens being irradiated in the Trojan Reactor cavity were machined from A212 grade B, A350 LF3, and A36 steels. The A212 grade B and A350 LF3 specimens were taken from HFIR archival materials to allow direct comparisons with existing data. The A36 specimens were included since it is a material which has been frequently used in pressure vessel supports. Five and six Charpy V-notch impact specimens from A36 and A212 grade B, respectively, in the L-T orientation were included. A holder, whose external dimensions are equal to that of a standard Charpy V-notch specimen, was designed, manufactured and assembled with 44 mini-tensile specimens. It contained an approximately equal number of mini-tensile specimens machined in the L orientation from each of the three materials mentioned above.

IN-SERVICE AGED MATERIAL EVALUATIONS

The primary objective of this task is to evaluate nuclear reactor components as a consequence of aging. The task focuses on directly examining structural components to allow for the assessment of actual material condition caused by exposure to normal or off-normal conditions.

The initial efforts under this task have addressed the assessment of existing facilities at ORNL and the establishment of supplementary facilities needed for conducting investigations of components removed from service. The examination of irradiated materials requires, of course, not only the usual mechanical property testing equipment, but facilities for determining physical properties and for detailed metallurgical studies, such as optical metallography, scanning electron fractography, and transmission electron microscopy. Also, machining of irradiated materials requires a remote machining operation in a hot cell or hot shop.

The efforts to date have focused on a detailed assessment of the extensive existing capabilities at ORNL for such examinations as well as individual deficiencies and courses of proposed action. The two items have been identified as most urgently needed. A remotely operated electrodischarge machining facility is required for efficient sectioning of activated materials and their fabrication into test specimens. An automated hardness tester is needed for screening of embrittlement on received components. Plans have been made and funding tentatively secured to obtain and install these items over the next two years.

CORRELATION MONITOR MATERIALS

Correlation monitor materials have been widely used to provide added confidence of the results of commercial power reactor surveillance capsule results. The recently approved revision the ASTM Standard Practice E 185 for Conducting Surveillance tests for Light-Water Cooled Nuclear Power Reactor Vessels now makes their use mandatory for the results to be considered credible. This increased need for and the recognition of decreasing supplies of suitable

correlation monitor materials were the bases for the establishment of a task with the specific goal of assuring an adequate supply of these materials for the foreseeable future.

Since two of the heavy-section plates procured in the early years of the HSST program, HSST plates 02 and 03, have been used for this purpose,[20] and moreover represent virtually all of the originally qualified correlation monitor material still available, the initial activity within this task is to prepare a detailed inventory of all remaining material from these plates and to establish an archival-quality storage facility in which to keep it. This effort was begun within the past year and is expected to be completed in 1993. In conjunction with archiving and maintaining custody of the material, the HSSI program has been authorized by the USNRC to release appropriately pedigreed correlation monitor material at no cost to qualified users who require it. In the past year, material has been supplied to General Electric for use in the BWR Owners Group Supplemental Surveillance Program and to Korean Heavy Industries for use in the surveillance program for Units 3 and 4 of the Yong Gwang pressurized water reactors.

SUMMARY

The HSSI program is actively involved in providing information in several technical areas regarding the irradiation embrittlement behavior of RPVs which is vital to their continued safe operation. In the HSSI Fifth and Sixth Irradiation Series, designed to examine the shifts and possible changes in shape in the ASME K_{Ic} and K_{Ia} curves for two irradiated high-copper welds, it was seen that both the lower bound and mean fracture toughness shifts were greater than those of the associated Charpy-impact energies, whereas the shifts in crack arrest toughness were comparable. The irradiation-shifted fracture toughness data fell slightly below the appropriately indexed ASME K_{Ic} curve even when it was shifted according to Revision 2 of Regulatory Guide 1.99 including its margins.

The beltline weld which was removed from the Midland reactor, fabricated by B&W using Linde 80 flux, is being examined in the Tenth Irradiation Series to establish the effects of irradiation on a commercial LUS weld. A wide variation in the unirradiated fracture properties of the Midland weld were measured with values of RT_{NDT} ranging from -22 to 54°F through its thickness. In addition, a wide range of copper content from 0.21 to 0.45 wt % was found, compared to the 0.42 wt % previously reported. The remainder of the unirradiated fracture testing and preparations for the irradiations of this material are under way.

Results from the Seventh Irradiation Series on stainless steel cladding have shown that the ductile fracture toughness initiation and tearing modulus of the cladding were significantly reduced by irradiation. The degree of reduction was such that post-irradiation ductile fracture resistance is as low or lower than comparably irradiated low upper-shelf weld metal.

Initial studies have shown that the time or dose required for the point defect concentrations, which ultimately contribute to irradiation embrittlement, to reach their steady state values can be comparable to the component lifetime or to the duration of an irradiation experiment. Thus, embrittlement models which rely on the assumption of steady state at these conditions are not valid. Consequently, simple direct comparisons of embrittlement generated under different rates of exposure (eg. test reactors vs power reactors) may be misleading because the relative state within the initial defect production transient will likely be different. Since the effect of displacement rate is different in the transient and steady state regimes, data extrapolation from test reactor irradiations may cross mechanism boundaries and lead to poor estimates of material response at low displacement rates.

A theoretical examination of the detailed irradiation mechanics which exist in low-temperature irradiations such as those which produced the accelerated embrittlement of the HFIR pressure vessel has led to the tentative conclusion that the cause of the acceleration is the high fraction of very low-energy thermal neutrons which existed rather than the low rate at which the fluence was accumulated. This conclusion is being investigated in two experiments. Specimens are being irradiated at low temperatures and high-fluence rates in spectra with and without large components of thermal neutrons. Other specimens are being exposed in the cavity of a pressurized water reactor at low temperatures and low fluence rates. As a result of the two experiments it should be possible to establish the mechanism primarily responsible for the accelerated low-temperature embrittlement.

Additional activities have been initiated which will provide for more detailed examination of the irradiation, annealing, and reirradiation response of LUS weldmetal, establish an improved facility for the examination of materials irradiated in service, and to assure a continuing source of supply for correlation monitor materials for use in light-water reactor surveillance programs.

ACKNOWLEDGMENTS

The author would like to acknowledge the numerous members of the Heavy-Section Steel Irradiation Program who contributed to the technical content of this work including C. A. Baldwin, K. Farrell, F. M. Haggag, S. K. Iskander, F. B. K. Kam, L. K. Mansur, D. E. McCabe, M. K. Miller, R. K. Nanstad, R. E. Stoller, K. R. Thoms, and J. A. Wang. In addition the author would like to thank A. Taboada, technical monitor of the program, and the rest of the U.S. Nuclear Regulatory Commission for the financial and technical support of this research effort.

REFERENCES

1. R. K. Nanstad et al, "Effects of Radiation on K_{Ic} Curves for High Copper Welds," pp. 214-233 in *Effects of Radiation on Materials: 14th International Symposium (Volume II)*, ASTM STP 1046, N. H. Packan, R. E. Stoller, and A. S. Kumar, Eds., American Society of Testing and Materials, Philadelphia, Pa., 1990.

2. W. R. Corwin, Martin Marietta Energy Systems, Inc., Oak Ridge Natl. Lab., Oak Ridge, Tenn., *Heavy-Section Steel Irradiation Program Semiannual Progress Report for October 1989-March 1990*, USNRC Report NUREG/CR-5591, Vol.1, No.1 (ORNL/TM-11568/V1&N1), August 1990.

3. *ASME Boiler and Pressure Vessel Code, An American National Standard*, Sect. XI, Appendix A, American Society of Mechanical Engineers, New York, 1986.

4. K. Wallin, "The Scatter in K_{Ic}-Results," *Engineering Fracture Mechanics*, **19**(6), 1085-93 (1984).

5. S. K. Iskander, W. R. Corwin, and R. K. Nanstad, Martin Marietta Energy Systems, Inc., Oak Ridge Natl. Lab., Oak Ridge, Tenn., *Results of Crack-Arrest Tests on Two Irradiated High-Copper Welds*, USNRC Report NUREG/CR-5584 (ORNL/TM-11575), December 1990.

6. W. R. Corwin, R. G. Berggren, and R. K. Nanstad, Martin Marietta Energy Systems, Inc., Oak Ridge Natl. Lab., Oak Ridge, Tenn., *Charpy Toughness and Tensile Properties of a Neutron Irradiated Stainless Steel Submerged-Arc Weld Cladding Overlay*, USNRC Report NUREG/CR-3927 (ORNL/TM-9709), September 1984.

7. F. M. Haggag, W. R. Corwin, D. J. Alexander, and R. K. Nanstad, "Tensile and Charpy Impact Behavior of an Irradiated Three-Wire Series-Arc Stainless Steel Cladding," pp. 361-372 in *Effects of Radiation on Materials: 14th International Symposium (Volume II)*, ASTM STP 1046, N. H. Packan, R. E. Stoller, and A. S. Kumar, Eds., American Society of Testing and Materials, Philadelphia, Pa., 1990.

8. F. M. Haggag, W. R. Corwin, and R. K. Nanstad, Martin Marietta Energy Systems, Inc., Oak Ridge Natl. Lab., Oak Ridge, Tenn., *Irradiation Effects on Strength and Toughness of Three-Wire Series-Arc Stainless-Steel Weld Overlay Cladding*, USNRC Report NUREG/CR-5511 (ORNL/TM-11439), February 1990.

9. A. L. Hiser, F. J. Loss, and B. H. Menke, Material Engineering Assoc., Lantham, Md., *J-R Curve Characterization of Irradiated Low Upper Shelf Welds*, USNRC Report NUREG/CR-3506, MEA-2028, April 1984.

10. J. J. McGowan, R. K. Nanstad, and K. R. Thoms, Martin Marietta Energy Systems, Inc., Oak Ridge Natl. Lab., Oak Ridge, Tenn., *Characterization of Irradiated Current-Practice Welds and A533 Grade B Class 1 Plate for Nuclear Pressure Vessel Service*, USNRC Report NUREG/CR-4880 Vols. 1 and 2 (ORNL/TM-6484/V1 and V2), July 1988.

11. R. K. Nanstad and R. G. Berggren, Martin Marietta Energy Systems, Inc., Oak Ridge Natl. Lab., Oak Ridge, Tenn., *Irradiation Effects on Charpy Impact and Tensile Properties of Low Upper-Shelf Welds, Heavy-Section Steel Irradiation Program, Irradiation Series 2 and 3*, USNRC Report NUREG/CR-5696
(ORNL/TM-11804), June 1991.

12. L. K. Mansur, American Nuclear Society Critical Reviews, *Nucl. Technol.* **40**, 5-34 (1978).

13. R. E. Stoller and G. R. Odette, "A Composite Model of Microstructural Evolution in Austenitic Stainless Steel Under Fast Neutron Irradiation," pp. 371-392 in *Radiation-Induced Changes in Microstructure: 13th International Symposium*, ASTM STP 955, F. A. Garner, N. H. Packan and A. S. Kumar, Eds., American Society of Testing and Materials, Philadelphia, Pa., 1987.

14. L. K. Mansur, "Irradiation Creep by Climb-Enabled Glide of Dislocations Resulting From Preferred Absorption of Point Defects" in *Phil. Mag. A* **39**, 497-506 (1979).

15. A. D. Brailsford and R. Bullough, AERE Harwell, UK, *The Theory of Sink Strengths*, AERE Harwell Report TP 854, 1980.

16. R. E. Stoller and L. K. Mansur, "The Influence of Displacement Rate on Damage Accumulation during the Point Defect Transient in Irradiated Materials," pp. 52-67 in *Proceedings of PM-90: International Conference on Radiation Materials Science, Vol. 1*, May 22-25, 1990, Alushta, The Crimea, USSR.

17. R. K. Nanstad, K. Farrell, D. N. Braski and W. R. Corwin, "Accelerated Neutron Embrittlement of Ferritic Steels at Very Low Damage Rate," J. Nucl. Mater. **158**, 1-6 (1988).

18. L. K. Mansur and K. Farrell, "On Mechanisms by Which a Soft Neutron Spectrum May Induce Accelerated Embrittlement," J. Nucl. Mater. **170**, 236—245 (1990).

19. L. K. Mansur and K. Farrell, "New Insights on Reactor Vessel Embrittlement," *Oak Ridge National Laboratory Review*, **22—4**, 30—35 (1989).

20. F. W. Stallman, Martin Marietta Energy Systems, Inc., Oak Ridge Natl. Lab., Oak Ridge, Tenn., *Analysis of A302B and A533B Standard Reference Materials in Surveillance Capsules of Commercial Power Reactors,* USNRC Report NUREG/CR-4947 (ORNL/TM-10459), January 1988.